Eur. Phys. J. B **20**, 321–333 (2001)

THE EUROPEAN PHYSICAL JOURNAL B

EDP Sciences

Microscopic interactions in $CuGeO_3$ and organic Spin-Peierls systems deduced from their pretransitional lattice fluctuations

J.-P. Pouget[a]

Laboratoire de Physique des Solides[b], Bâtiment 510, Université de Paris Sud, 91505 Orsay, France
and
Département Sciences Physiques et Mathématiques, CNRS, 3 rue Michel-Ange 75794 Paris, France

Received 13 September 2000 and Received in final form 6 February 2001

Abstract. $CuGeO_3$ exhibits a Spin-Peierls (SP) transition, at $T_{SP} = 14.3$ K, which is announced above 19 K by an important regime of one-dimensional (1D) pretransitional lattice fluctuations which can be detected until about 40 K using X-ray diffuse scattering investigations. A quantitative analysis of this scattering shows that in this 1D direction the correlation length follows the "universal" behaviour expected for the thermal fluctuations of a real order parameter which characterizes the lattice dimerization. This allows to define a 1D mean-field temperature, T_{SP}^{MF}, of about 60 K and invalidates any mean field scenario for the SP transition of $CuGeO_3$. As T_{SP}^{MF} is as high as $4T_{SP}$ we propose that the 3D-SP order is achieved by the interchain coupling between 1D solitons which form below about 16–20 K. $CuGeO_3$ being in the non-adiabatic regime, it is also suggested that the observed pretransitional fluctuations of $CuGeO_3$ originate from the X-ray scattering on a very broad damped critical response of lower frequency than the "critical" phonon modes. From the quantitative analysis of the 1D fluctuations we also estimate the microscopic parameters of the SP chain. These parameters allow to locate $CuGeO_3$ close to the quantum critical boundary separating the gapped SP ground state to the ungapped anti-ferromagnetic ground state. The vicinity of a quantum critical point emphasizes the role of the quantum and non-adiabatic fluctuations and the importance of the interchain coupling in the physics of $CuGeO_3$. Finally we compare these findings with those obtained for the organic SP systems $(BCPTTF)_2PF_6$, $(TMTTF)_2PF_6$ and $MEM(TCNQ)_2$. From a similar analysis of the pretransitional lattice fluctuations it is found that $(BCPTTF)_2PF_6$ and $(TMTTF)_2PF_6$ are located on the SP gapped classical-quantum boundary and are in the adiabatic regime where the fluctuations lead to the formation of a pseudo-gap in the spin degrees of freedom. Differently, we place $MEM(TCNQ)_2$ inside the SP quantum phase around the crossover line between the adiabatic and non-adiabatic regimes.

PACS. 71.27.+a Strongly correlated electron systems; heavy fermions – 71.10.pm Fermions in reduced dimensions (anyons, composite fermions, Luttinger liquid, etc.)

1 Introduction

A remarkable feature of correlated one-dimensional (1D) electronic systems is the occurrence of a spin-charge decoupling when the electrons undergo strong enough Coulomb repulsions. This is achieved for any finite value of the intrasite Coulomb repulsion, U, at half band filling ($\rho = 1$ electron per site) and for others band fillings when there are long range enough Coulomb repulsions [1,2]. In this latter case the charge degrees of freedoms condense into a 1D-$4k_F$ charge density wave (CDW)-Wigner lattice which modulation wave vector is $\rho G_\parallel$, where ρ is the average number of electron per site and $G_\parallel = 2\pi/c$ is the 1D lattice's reciprocal wave vector unit. Strong Coulomb repulsions thus lead, in the Mott-Hubbard ($\rho = 1$) and Wigner-CDW (for simple commensurate ρ values such as 1/2) cases, to an insulating ground state protected by an energy gap Δ_ρ from the individual charge excitations. This charge localisation does not affect the spin degrees of freedom whose excitation spectrum remain gapless. In absence of orbital degeneracy, the exchange interaction generally favors the antiferromagnetic (AF) coupling between near neighbour $S = 1/2$ spins. In absence of anisotropy and in the localized limit the interacting $S = 1/2$ chain is described by the Heisenberg Hamiltonian, with the exchange constant J_{nn}. Below $k_B T_\sigma \approx 0.64 J_{nn}$, when the magnetic coherence length:

$$\xi_{AF}(T) \approx \hbar v_\sigma / \pi k_B T, \quad (1)$$

[a] e-mail: pouget@lps.u-psud.fr
[b] CNRS-UMR 8502

whose spin velocity is given by $\hbar v_\sigma = \pi J_{nn} c/2$, becomes larger than the interspin distance c, AF (if $\rho = 1$) or $2k_F$ spin density wave (SDW) (if $\rho \neq 1$) correlations develop. However, as pointed out by Anderson [3], an important fraction of the ground state fluctuations of the $S = 1/2$ AF Heisenberg chain contains non magnetic singlet components. These components can be picked out of the quantum fluctuations in presence of an important spin-phonon coupling allowing the $S = 1/2$ AF chain to dimerize [4]. The dimerization forms a lattice of non-magnetic $S = 0$ singlet pairs whose magnetic excitations are separated from the ground state by energy gaps [5]. The Spin Peierls (SP) ground state can be viewed as the magnetic analog of the $2k_F$ CDW-Peierls ground state observed in 1D conducting systems [6]. The SP dimerization order parameter has thus the same symmetry as the $2k_F$ CDW-Peierls bond order parameter (or bond order wave (BOW) parameter) of the half-filled band metal ($\rho = 1$). Thus by increasing the electron-electron repulsions one passes continuously from a $2k_F$ BOW-Peierls ground state to a SP ground state. In the literature the SP transition has been mainly considered in the localized limit which assumes that Δ_ρ is much larger than the SP gap, Δ_σ. The consideration of delocalization effects leads to corrections at the Heisenberg Hamiltonian and thus at the mechanism of the SP transition [4,7].

At $T = 0$ K the isolated SP chain undergoes a long range dimerization when the spin-phonon coupling, α, exceeds a critical value α_c. α_c depends upon J_{nn} and Ω_0, the bare frequency of the critical phonon mode of the SP transition. α_c has about the same value for the XY [8] and the Heisenberg [9,10,67] SP chains. For $\alpha < \alpha_c$ the SP order is destroyed by the quantum fluctuations. For α slightly larger than α_c a quantum-classical crossover occurs when the spin-Peierls gap, Δ_σ, is of the order of Ω_0. At larger values of α, in the classical regime where $\Delta_\sigma > \Omega_0$, the spin-Peierls gap still remains renormalized with respect to its mean field value (*i.e.* $\Delta_\sigma < \Delta_\sigma^{MF}$, which will be defined in Sect. 2) by the non-adiabatic corrections of the phonon field [8]. As the Heisenberg $S = 1/2$ Hamiltonian is spin-rotationally invariant the quantum fluctuations of the phase of the order parameter destroy the AF or the SDW long range order even at $T = 0$ K. Thus the study of the competition between the magnetic and SP orders observed in several experimental systems requires the consideration of the interchain coupling: *i.e.* the exchange coupling between neighbouring chains of spins, for the magnetic order, and the Coulomb coupling between neighbouring chains of charged dimers, for the SP order.

The first example of dimerisation of a Heisenberg chain was found for the V^{4+} zigzag chains of stressed or substituted VO_2 [11]. Then the SP transition has been observed both in half-filled ($\rho = 1$) and in quarter-filled band ($\rho = 1/2$) systems. Typical $\rho = 1$ SP systems are TTF-CuBDT [12] and $CuGeO_3$ [13]. Typical $\rho = 1/2$ SP systems are the organic salts: $MEM(TCNQ)_2$ [14], $(TMTTF)_2X$ [15–17] and $(BCTTTF)_2X$ [18], with X= PF_6 and AsF_6. A SP transition has also been reported in the $\rho = 1/2$ system α'-NaV_2O_5 [19]. However as the vanadates are made of parallel ladders and zigzag chains coupled in a trellis lattice one expects a complex transition with the coexistence of CDW and SP orders [20]. As the $4k_F$ charge localisation wave is centered either on the sites or on the bonds of the chain, the $\rho = 1/2$ systems exhibit a richer phase diagram than the $\rho = 1$ systems. In the former systems the dimerization of each kind of $4k_F$ CDW lattices leads to a SP ground state with different symmetry [21,22]. These SP orders compete also with different magnetic phases when the magnetic interchain coupling is considered [23]. Competition between SP and AF/SDW orders has been reported in the $(TMTTF)_2X$ family and in substituted $CuGeO_3$.

As previously found for the half-filled band Peierls systems, such as the polyacetylene [24], the SP dimerized ground state is doubly degenerate. One passes from one ground state to the other by changing the phase of the dimerisation by π. This is achieved through a defect of dimerization, spatially localized on ξ_S, called a soliton. As this defect leaves one unpaired site, each soliton bears a spin 1/2. The solitons are the elementary defects of the dimerized chain. They are thermally excited and are responsible, below about $T_{SP}^{MF}/4$, to the break of the long range dimerization order of the isolated SP chain at finite temperature [25,26] (T_{SP}^{MF} is the mean field temperature of the chain which will be defined in Sect. 3). Magnetic solitons are also induced when the SP chain is polarized by an external magnetic field, H. Its effect, which is analogous to that caused by a variation of the band filling of the Peierls chain from half filling [27,28], leads, after a 1st order phase transition, to an incommensurate modulated phase made of equispaced solitons which density increases with H [29]. Solitons are also created by any kind of structural defect breaking the SP order [30].

All these considerations show that the underlying physics of the SP instability is of 1D nature. However until now the SP transition of $CuGeO_3$ has only been described within the RPA-mean field approximation [31–35]. It is however well known, especially from the study of Peierls systems [36], that such an analysis is not valid for 1D systems or 3D anisotropic systems presenting an important regime of 1D fluctuations. The purpose of this paper is thus to analyse quantitatively previously published X-ray diffuse scattering data [37,38] in order to stress the importance of 1D lattice fluctuations in the SP transition of $CuGeO_3$ and to make the link with the organic $(TMTTF)_2X$ and $(BCTTTF)_2X$ SP systems [15,18,26] which behave similarly. In part II of this paper we shall summarize several features of the SP transition of pure $CuGeO_3$ which do not have received a satisfactory explanation until now. In Section 3 the pretransitional X-ray fluctuations will be quantitatively analyzed and their dynamics will be discussed in relationship with the neutron scattering data in Section 4. Finally, in Section 5, these findings will be compared to those found in the organic SP and Peierls systems. Additional concluding remarks will be presented in Section 6.

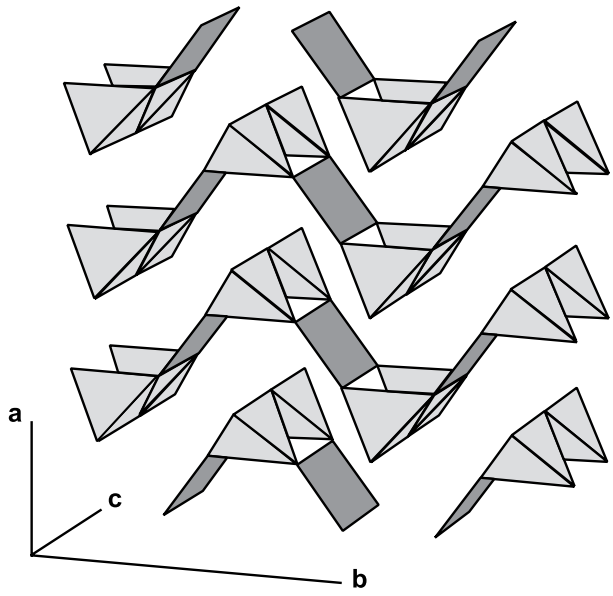

Fig. 1. Schematic representation of the structure of $CuGeO_3$ showing the bonding network between the CuO_2 squares and the GeO_4 tetrahedra. The O(2) atoms are shared between the squares and the tetrahedra and the O(1) atoms are only shared between the tetrahedra.

2 The Spin-Peierls transition of $CuGeO_3$

Figure 1 shows the anisotropic bonding network of the orthorhombic (Pbmm) high temperature structure of $CuGeO_3$. The magnetic $S = 1/2$ Cu^{2+} surrounded by a square of oxygen atoms, denoted O(2) below, forms ribbons running along the c-direction. These ribbons are linked together in a zigzag manner with GeO_4 tetrahedra along the b-direction. The linkage with the others GeO_4 tetrahedra through elongated Cu-O(1) distances is weaker in the a direction.

$CuGeO_3$ undergoes a 2nd order SP transition at $T_{SP} = 14.3$ K revealed by a continuous drop of the spin susceptibility [13] and a progressive lattice dimerisation [37,39]. Structural refinements performed below T_{SP} [40,41] show a complex distortion pattern involving mostly two normal modes of deformation characterized by (i) a dimerisation along c of the Cu chains together with a modulation of the O(2)-O(2) edge lengths perpendicular to c [$(T_2^+)_1$ mode] and (ii) a twisting of the CuO_2 ribbons in the ab-plane [$(T_2^+)_2$ mode]. The associated atomic displacements modulate the exchange integrals through variation of the angles of the Cu-O(2)-Cu superexchange path. J_{nn} is affected both by the $(T_2^+)_1$ Cu displacement, which changes the Cu-O(2)-Cu angle, and by the $(T_2^+)_2$ O(2)-O(2) tilting, which changes the O-Ge hybridization through the variation of the O(2)-O(2)-Ge angle [31]. The $(T_2^+)_2$ tilting changes also the Cu-O(2)-O(2)-Cu superexchange path involved in the next near neighbour exchange integral J_{nnn} which will be introduced below.

The SP transition forms a singlet-triplet gap, Δ_σ, in the magnetic excitation spectrum the value of which varies with the reciprocal wave vector from 23 K ([0,1,1/2]: position of the AF superlattice reflection in substituted $CuGeO_3$) to 66 K ([1/2,0,1/2]: position of the SP reflection) [42]. The scaling of the lowest value of the energy gap, 23 K, with the critical SP temperature, $T_{SP} = 14.3$ K, *via* the BCS-like relationship [43]:

$$2\Delta_\sigma^{MF} \approx 3.1 k_B T_{SP}^{MF}, \quad (2)$$

was considered in the literature as the proof that the SP transition of $CuGeO_3$ is mean-field like with respect to the lattice degrees of freedom. In fact this equality does not hold under pressure because the rate of increase of the lowest value of the energy gap ($d\mathrm{Log}\Delta_\sigma/dP$=65%/GPa) is more than two times larger than that of the SP critical temperature ($d\mathrm{Log}T_{SP}/dP$=25%/GPa) [44]. In addition the use of the relationship (2) with a gap value taken at a reciprocal position different from that of the SP critical wave vector is misleading. If, the average spin gap value of 45 K is used in the relationship (2), a T_{SP}^{MF} two times larger than T_{SP} is thus obtained. Also numerical simulations of the SP-XY [8] and Heisenberg [10,45,46] models show that when the finite value of the bare frequency, Ω_0, of the critical phonon mode is taken into account the singlet-triplet gap Δ_σ can be sizeably reduced with respect to its mean field value Δ_σ^{MF}; Δ_σ^{MF} corresponds to the $T = 0$ K SP gap in the extreme adiabatic limit (*i.e.* in the limit $\Omega_0 \to 0$).

A surprising behaviour of $CuGeO_3$ was the measurement above T_{SP} of a spin susceptibility which does not follow the Bonner and Fischer thermal behaviour expected for a $S = 1/2$ near neighbour AF Heisenberg chain. It was however soon realized [47,48] that the thermal behaviour of the spin susceptibility of $CuGeO_3$ can be correctly reproduced if one introduces a next near neighbour AF exchange interaction J_{nnn}. The best fit of the spin susceptibility of $CuGeO_3$ thus leads to $J_{nn} = 160$ K and $J_{nn}/J_{nnn} = 0.35$ [49]. With such a high J_{nn}/J_{nnn} ratio, exceeding the critical value 0.241, the spin chain is frustrated, which means that it should exhibit a finite gap in the spin degrees of freedom even in absence of any dimerisation. It was thus proposed that the frustration effects are the driving force achieving the non magnetic ground state of $CuGeO_3$ [50,51]. However numerical calculations show that with the above quoted value of the exchange constants the spin gap resulting from the frustration effects is only of 2.4 K [52], *i.e.* more than one order of magnitude smaller than the experimental gap. The spin gap thus observed in $CuGeO_3$ results from the lattice dimerization and not from a pure effect of frustration of the magnetic interactions. In addition it has been already pointed out in the literature [53] that the non-adiabatic coupling of the magnetic degrees of freedom to the phonon field can induce such a frustration effect. In this respect it has been also shown that the consideration of a sizeable spin-phonon coupling in the Heisenberg Hamiltonian leads also to a deviation of the spin susceptibility from the Bonner and Fisher behaviour [54].

All these features point toward a non standard scenario for the SP transition of $CuGeO_3$. Thus a reexamination

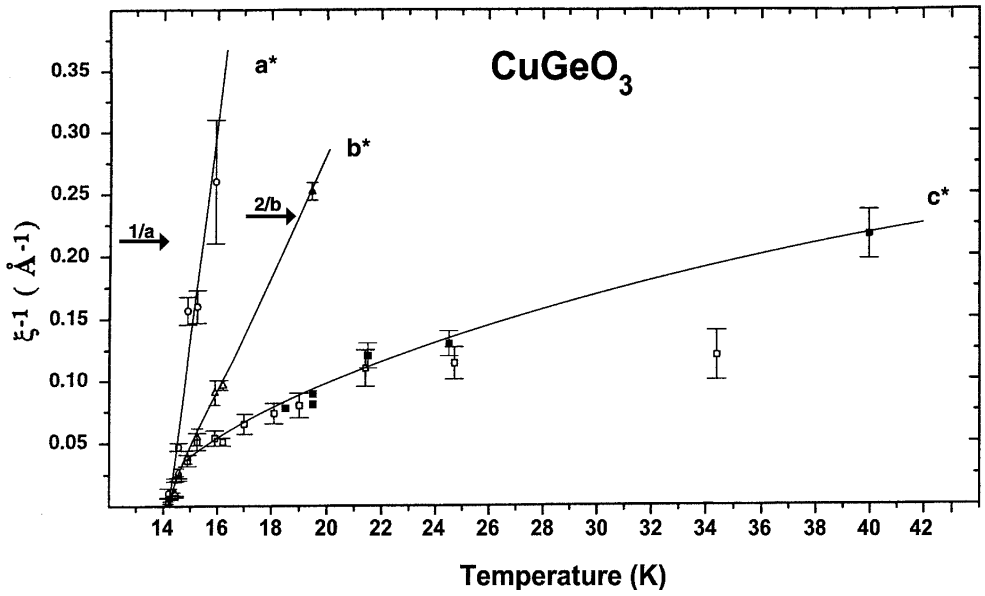

Fig. 2. Thermal dependence of the inverse correlation length in the a, b and c (chain) directions of $CuGeO_3$. The filled symbols are from the photographic investigation of reference [37] and the empty ones from the diffractometric investigation of reference [38]. The inverse interchain distances $1/a$ and $2/b$ are also indicated.

of the mechanism of transition requires a clarification of the role of the lattice fluctuations and of the dynamics of the associated phonon field. These topics are the object of the next two parts.

3 The pretransitional fluctuations

The SP transition of $CuGeO_3$ is announced by an important regime of pretransitional fluctuations whose structural counterpart has been detected up to 40 K [37,38] by X-ray diffuse scattering. It is also important to precise that the X-ray scattering is mostly sensitive to the dimerisation of the Cu atoms involved in the $(T_2^+)_1$ mode and that this mode has the strongest spin-phonon coupling, according to the analysis of reference [31]. The fluctuations measured by this technics thus probe the Cu lattice degrees of freedom. Figure 2 gives above T_{SP} the thermal variation of the inverse correlation length in the a, b and c principal directions. Below 16 K, the thermal variation of ξ_c^{-1} is in very good agreement with that of ξ_c^{-1} deduced from the width of the central peak observed by elastic neutron scattering [35a,55]. The thermal variation of ξ_a^{-1} agrees also with that of the synchrotron X-ray scattering study of reference [56].

The inverse correlation length anisotropy, $\xi_c > \xi_b > \xi_a$, reflects the structural anisotropy. More quantitatively the anisotropy ratio is at 16 K, the crossover temperature to the regime of 2D fluctuations, of $\xi_c : \xi_b : \xi_a = 5 : 3 : 1$. This ratio is comparable to that of the short length scale fluctuations, 7 : 2.5 : 1, measured in the vicinity of T_{SP} by synchrotron X-ray scattering [57]. The anisotropy ratio of the correlation lengths of $CuGeO_3$ is slightly larger than the one found in others SP systems such as $(BCPTTF)_2AsF_6$ (3.6 : 2.6 : 1) [18] and α'-NaV_2O_5 (3.8 : 1.8 : 1) [58]. In all these compounds the longest correlation length is in the chain direction, as expected for a transition driven by the magnetic subsystem. As far as the pretransitional fluctuations are concerned $MEM(TCNQ)_2$ shows a quite different behaviour with, in the critical regime near T_{SP}, an interchain correlation length longer than the intrachain one [18]. This inverted anisotropy shows that the SP instability of $MEM(TCNQ)_2$ is driven by a different mechanism. It has been suggested [59] that, as well as in TTF-CuBDT, the SP instability of $MEM(TCNQ)_2$ is driven by a pre-existing soft lattice mode.

A comparison of the $\xi_i(T)$'s of $CuGeO_3$ with the interchain distances (a and $b/2$) allows to define the crossover temperatures at which the dimensionality of the fluctuations is reduced. Figure 2 shows that ξ_a amounts the interchain distance, a, at 15.5 K (at 16.5 K from the data of Ref. [56]) and that ξ_b amounts the interchain distance, $b/2$, at 19 K. Thus between T_{SP} and about 16 K the fluctuations are 3D, then 2D (in the bc-plane) until 19 K. The elastic quantities exhibit a change in their thermal variations around these crossover temperatures. The critical divergence of the thermal expansion along b begins to start in the regime of 2D fluctuations, while that along a and c is detected in the regime of 3D fluctuations [60]. Below 19 K, in the regime of 2D fluctuations, there is a deviation from the linear rate of increase of the C_{33} elastic constant followed by a well pronounced sound velocity softening [61].

A sizeable regime of 1D structural fluctuations takes place above 19 K, as already pointed out in our first

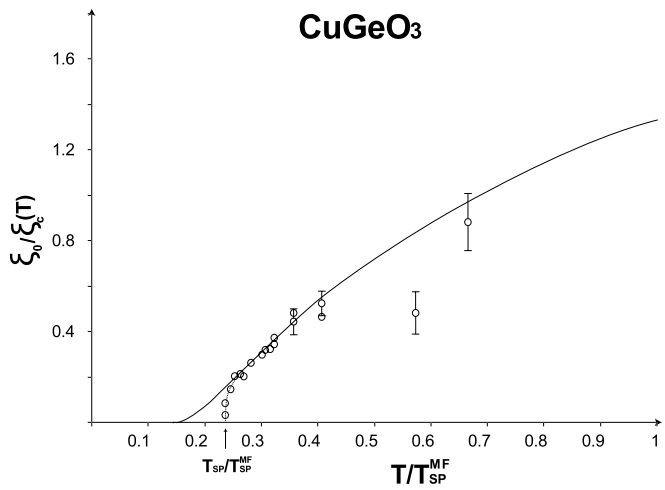

Fig. 3. Thermal dependence of the inverse reduced interchain correlation length $\xi_0/\xi_c(T)$ in function of the reduced temperature $T/T_{\rm SP}^{\rm MF}$. The solid line represents the exact calculation of the thermal dependence of the inverse correlation length of a real order parameter in 1D [26]. The 3D SP critical temperature of $CuGeO_3$, $T_{\rm SP}$, is also indicated.

report [37]. This behaviour is expected when the SP instability is triggered by the 1D AF correlations. In this respect Figure 3 shows that above 15.5 K the thermal dependence of the inverse intrachain correlation length, ξ_c^{-1}, of $CuGeO_3$ can be well accounted for the exact calculation of the1D fluctuations for a real order parameter, which is of the relevant symmetry to describe the SP dimerization. This calculation, using the transfer matrix method applied to the Landau-Ginzburg functional, shows [25] that there are two regimes of fluctuations:

- above $0.4\,T_{\rm SP}^{\rm MF}$, a regime of renormalized Gaussian fluctuations, where:

$$(\xi_c/\xi_0)^{-1} \approx [(T/T_{\rm eff}) - 1]^{1/2}, \quad \text{with } T_{\rm eff} \approx 0.3\,T_{\rm SP}^{\rm MF}, \tag{3}$$

- below about 0.2–$0.3T_{\rm SP}^{\rm MF}$, a regime of thermal excitations of domain walls (solitons) which cut the SP chain into ordered domains whose inverse size is given by:

$$(\xi_c/\xi_0)^{-1} \approx (2T_{\rm SP}^{\rm MF}/T)\exp -(aT_{\rm MF}^{\rm SP}/T), \quad \text{with } a \approx 0.92. \tag{4}$$

In these expressions, $\xi_0 = \xi_{\rm AF}(T_{\rm SP}^{\rm MF})$ is given by (1) and $T_{\rm SP}^{\rm MF}$ is the temperature at which the coefficient of the second order term of the Landau-Ginzburg functional vanishes.

These two regimes are separated, at about $T_{\rm SP}^{\rm MF}/3$, by an inflection point in the thermal dependence of ξ_c^{-1}. In $CuGeO_3$ this inflection point can be guessed around 20 K. This location leads to a mean field temperature, $T_{\rm SP}^{\rm MF}$, of about 60 K. The scaling of the experimental results with the 1D calculation allows to fix the SP coherence length ξ_0 at 4 Å. This leads, with $T_{\rm SP}^{\rm MF} = 60$ K, to a near neighbour exchange integral of $J_{nn} = 160$ K, which value agrees quite well with that reported in the literature [49]. Figure 3 indicates that at $T_{\rm SP}^{\rm MF}\xi_c$ amounts at 3 Å, the interspin distance. $T_{\rm SP}^{\rm MF}$ is thus the temperature at which the 1D-SP fluctuations begin to develop by coupling the first neighbouring spins. The same physics was found in the organic SP compound $(BCPTTF)_2\,AsF_6$ [26]. In reference [35a], the thermal dependence of our experimental ξ_c^{-1} was fitted using a RPA treatment of the SP transition of $CuGeO_3$. The agreement is poorer than the one shown Figure 3.

It is particularly interesting to remark that $T_{\rm SP}^{\rm MF}$ corresponds at about the temperature, 55 K, at which the spin susceptibility exhibits a maximum [13,37,49]. This indicates that the SP structural correlations develop conjointly with the growth of the 1D-AF short range order [50]. Such a synchronous behaviour can be understood if the magnetic and SP fluctuations are linked by a sizeable spin-phonon coupling ($\alpha \sim J_{nn}$), in agreement with the literature [45,46]. The occurrence of a sizeable magnetoelastic coupling between the elastic and magnetic degrees of freedom of $CuGeO_3$ is also sustained by the thermal behaviour of the lattice expansion coefficients, α_i', which exhibit a sizeable anomalies around 60 K under the form of an extremum for α_a' and α_c' and of a change of slope for α_b' [60]. The thermal variation of the a and c lattice parameters changes in an opposite manner the Cu-O(2)-Cu angle which is the basic deformation of the $(T_2^+)_1$ critical mode. The thermal variation of b modifies the O(2)-O(2)-Cu angle which is the basic deformation of the $(T_2^+)_2$ critical mode, where the twisting of the CuO_2 ribbons is correlated with a displacement of the GeO_4 tetrahedra along b.

The intrachain correlation length measurements show that around $T_{\rm SP}^{\rm MF}/3 \sim 20$ K there is a crossover from the renormalized Gaussian regime to the regime of thermal excitation of solitons. This corresponds also at about the temperature at which the interchain coupling along b is set. The solitons are in fact well defined only below 16 K when ξ_c becomes larger than the soliton width $\xi_{\rm S}(\sim 20$ Å according to the NMR measurements [62]). At this temperature the weakest interchain coupling along a becomes also relevant and the 3D critical regime starts. It thus appears that the 3D-SP transition, which occurs at about $T_{\rm SP}^{\rm MF}/4$ in $CuGeO_3$, is driven by the interchain coupling between the just formed 1D solitons. The interchain coupling between solitons could provide the suitable explanation of the great sensitivity of the SP transition to the disorder. Thus the large drop of the SP critical temperature $T_{\rm SP}$ observed in substituted $CuGeO_3$ could be achieved by the pinning of solitons on the substituents. In this respect it is interesting to note that the typical size of the non 3D ordered SP domains observed in substituted $CuGeO_3$, $\pi\xi_c^{\rm D}(\sim 60$ Å in weakly substituted Si solid solutions [38]), is comparable to the soliton size $2\xi_{\rm S}$. This point will be addressed in a companion paper [63].

4 Dynamics of the fluctuations

$CuGeO_3$ develops pretransitional fluctuations on a large temperature range of about 2–3 times T_{SP}, as usual for 1D systems where the onset of 3D order is conditioned, for a weak interchain coupling, by the development of a long enough intrachain correlation length (until the formation of solitons in the present case). X-ray diffuse scattering experiments, which integrates in energy these fluctuations, give only "thermodynamical" informations, but does not provide any information on the dynamics of the fluctuations. A combined discussion with the inelastic neutron scattering results is thus necessary in order to precise the microscopic mechanism of the phase transition.

Inelastic neutron scattering measurements reveal that the phonons associated to the $(T_2^+)_1$ and $(T_2^+)_2$ critical modes have a quite high frequency, of 310 K and 150 K respectively [64]. The first surprise is to found two critical modes for a single structural transition. The simplest explanation is that the real critical mode is the $(T_2^+)_1$ mode of dimerisation of the Cu chains of higher energy (this mode has the strongest spin-phonon coupling, according to the analysis of Ref. [31]). Its instability drives that of the $(T_2^+)_2$ mode of same symmetry but of lower frequency. The second surprise is that the frequency of these two modes does not soften when the temperature decreases (a slight hardening of their frequency is even observed). The only critical effect that has been observed until now from the various neutron scattering investigations is the growth of a central peak in energy below about 16 K, in the regime of 3D fluctuations [55]. The onset of a central peak, which signals the slow dynamics of "heavy" objects, is consistent with the presence of solitons. Consistently, the central peak is observed in the temperature range where solitons are formed according to our interpretation of the thermal dependence of ξ_c. However we have performed in reference [38] a comparison of the X-ray diffuse scattering intensity with that of the elastic neutron scattering which shows that above T_{SP} most of the X-ray pretransitional intensity has an inelastic component. This inelastic structural component, which should be observed until about T_{SP}^{MF}, has not yet be detected by neutron scattering (see note added in proof). Its detection should be particularly difficult because of its overlap or mixing with the continuum of AF excitations [64]. However a recent detection of interferences in the polarized neutron inelastic scattering from $CuGeO_3$ [65] shows the presence of composite spin-lattice excitations, on an energy range of at least $k_B T_{SP}^{MF}$, below and above T_{SP}.

The understanding of the pretransitional dynamics of the SP transition thus requires the complete calculation of the frequency and thermal dependences of the phonon spectral function including the 1D fluctuations. Such a calculation has not yet be performed. A qualitative description, neglecting the low dimensional structural fluctuations, can be obtained from a RPA treatment of the spin-phonon coupling. Such an analysis has recently be performed for the exactly solvable XY model of the SP transition [35]. For the Heisenberg model, more relevant to describe the SP instability of $CuGeO_3$, an analytic derivation has been done in the adiabatic regime [33] and a numerical simulation was performed whatever the respective values of T_{SP}^{MF} and Ω_0 [66]. Below we shall summarize the main results of this last study which qualitatively accounts for the first time of all the observations performed in $CuGeO_3$. Figure 4 gives in reduced scales the temperature (T/T_{SP}^{MF}) and frequency (ω/Ω_0) dependences of the imaginary part of the retarded phonon propagator at the critical wave vector q_{SP}, Im $D(q_{SP}, \omega)$, for different values of T_{SP}^{MF}/Ω_0. This quantity is simply related to the SP phonon spectral function, $S(q_{SP}, |\omega|)$ by the relationship:

$$S(q_{SP}, |\omega|) = \coth(\hbar|\omega|/2k_B T)\text{Im } D(q_{SP}, \omega). \qquad (5)$$

In the adiabatic regime, for $T_{SP}^{MF} \geq \Omega_0$ (Figs. 4a and b), there is a soft phonon dynamics, where the frequency of a well defined critical phonon mode vanishes at T_{SP}^{MF}. In this regime the softening of the frequency of the critical phonon is mean field like [33]. In the extreme non-adiabatic regime, for $T_{SP}^{MF} \ll \Omega_0$ (Fig. 4d), only a well defined central peak exhibits a critical growth together with a critical sharpening as the temperature tends to T_{SP}^{MF} (the same result is shown Fig. 8 in Ref. [35a]). The frequency of the phonon mode, which was critical for $T_{SP}^{MF} \geq \Omega_0$, stays constant at Ω_0 in temperature. There is thus a complete decoupling between the low and high frequencies parts of the spectral function. It was found reference [33] that, in the RPA approximation, there is no more softening when the ratio T_{SP}^{MF}/Ω_0 is lower than $R_c = 0.46$. In the case where T_{SP}^{MF} is less than $R_c\Omega_0$, the phonon spectral function exhibits a quite complex frequency dependence which has not yet be described in detail. Numerical simulations reported Figure 4c shows the thermal dependence of the spectrum for $T_{SP}^{MF} = 0.2\Omega_0$, which corresponds, according to our determination of $T_{SP}^{MF} = 60$ K, to the case of $CuGeO_3$ (we take also $\Omega_0 = 310$ K, assuming that the most critical phonon mode is $(T_2^+)_1$). When the temperature decreases the intensity of the low frequency range of the spectrum grows critically, while the intensity of its larger frequency range gently decreases. The overdamped and critical nature of the low frequency part of phonon spectrum results from the mixing of the lattice degrees of freedom with the spin excitations. We think that this is the critical growth of the low frequency part of the phonon spectrum, which extents on a frequency range of about $\Omega_0/2$, which gives rise, by frequency integration, to the observed critical X-ray diffuse scattering (this quantity is proportional to $S(q_{SP}, t = 0)$, the $t = 0$ Fourier transform of $S(q_{SP}, \omega)$ given by the expression (5)). In the high frequency part of the spectrum the "critical" phonon mode hardens as the temperature decreases. The phonon mode hardening, already found in reference [33], could be due to a reduction of the "screening" of the phonon frequency by the gapping of the continuum of magnetic excitations. It has been observed in $CuGeO_3$ below about 120 K $\sim 2T_{SP}^{MF}$ [64]. Note that if T_{SP}^{MF} is taken equal at T_{SP}, as it is done in reference [35], $CuGeO_3$ would correspond to the situation depicted Figure 4d which does not exhibit the phonon hardening effect.

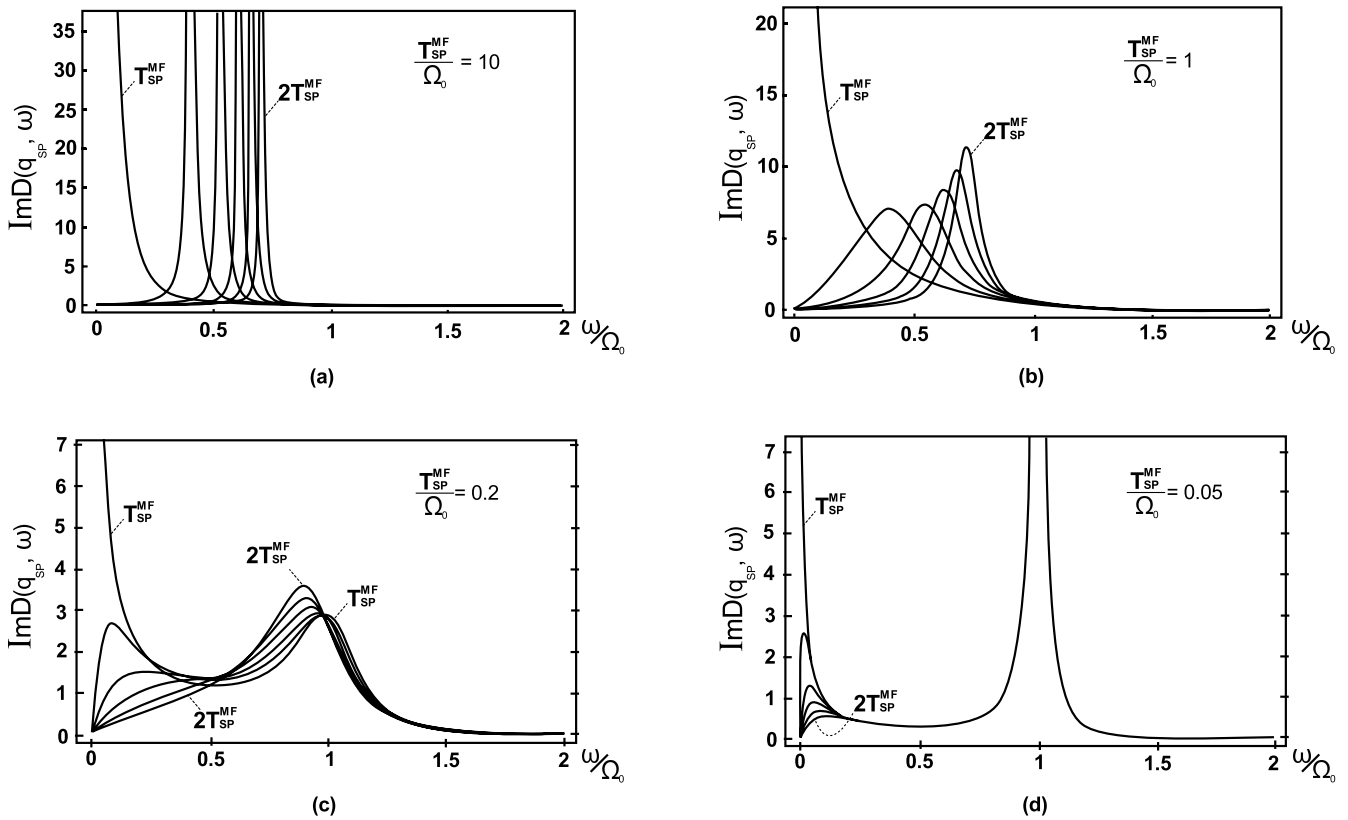

Fig. 4. RPA calculation of the reduced frequency (ω/Ω_0) dependence of the imaginary part of the retarded critical phonon propagator, Im $D(q_{\rm SP},\omega)$, for different values of $T_{\rm SP}^{\rm MF}/\Omega_0$: 10 (a), 1 (b), 0.2 (c) and 0.05 (d), and represented between $T_{\rm SP}^{\rm MF}$ and $2T_{\rm SP}^{\rm MF}$ by step of 0.2 $T_{\rm SP}^{\rm MF}$ (from Ref. [66]).

In presence of 1D fluctuations and in the classical SP regime, for $\alpha \gg \alpha_{\rm c}$, it is expected, by analogy with the treatment of the classical Peierls chain [68], that the concept of soft mode remains valid. But, as there is no SP transition at finite temperature in 1D, the frequency softening will continue below $T_{\rm SP}^{\rm MF}$ in the renormalized Gaussian regime previously introduced. However one expects to observe below $T_{\rm eff}$ (defined in expression (3)), in the solitonic regime, the growth of a central peak. For $\alpha \geq \alpha_{\rm c}$, the low energy part of the spectral function will still be conditioned by the presence of solitons. The dynamics associated to the formation of solitons which connect doubling degenerate states, whose phase of the dimerisation differs by π, is of the order-disorder type. In this respect, it has been shown [9] that at $T = 0$ K the phonon spectral function keeps a divergent weight extending to zero frequency (central peak) whatever α. However for $\alpha < \alpha_{\rm c}$, when there is no SP ground state, the phonon spectral function presents an energy gap with the central peak. It's only for $\alpha > \alpha_{\rm c}$, when the SP gap develops at $T = 0$ K, that the phonon spectral function exhibits a continuum between the central peak and the "critical" phonon mode, as found in the RPA calculation.

Although the RPA calculation qualitatively accounts for the shape of the spectral function, a detailed analysis must take into account the fluctuations leading to the formation of solitons which occurs below about 20–16 K in $CuGeO_3$, according to the conclusions of Section 3. This effect is all the more important that we shall suggest, in the next section, that $CuGeO_3$ is close to the ungapped quantum limit.

5 Comparison with organic Spin-Peierls and Peierls systems

5.1 Adiabaticity

Table 1 gives the 3D critical temperature ($T_{\rm SP}$) of various SP systems, their 3D spin gap (Δ_σ), the temperature ($T_{\rm F}$) at which the 1D fluctuations start (except for MEM(TCNQ)2 where $T_{\rm F}$ corresponds at the start of the 3D critical fluctuations [18]), the mean field gap calculated from the expression (2) assuming that $T_{\rm F} = T_{\rm SP}^{\rm MF}$, the bare frequency of the phonon mode associated to the SP instability (Ω_0) and finally the near neighbour exchange interaction (J_{nn}) deduced from a fit of the thermal dependence of the spin susceptibility (in the case of $CuGeO_3$ the best fit leads also to a next near neighbour exchange interaction J_{nnn} [49] which is not reported in the table). Table 1 compares also these SP systems with two different Peierls systems. In these Peierls systems the gap Δ occurs in both

Table 1. 3D-SP critical temperature T_{SP}, temperature at which the 1D fluctuations start T_F, 3D-SP gap Δ_σ, mean field gap Δ_σ^{MF} (given by the expression (2)), bare phonon frequency Ω_0, near neighbour exchange integral J_{nn}, SP coherence length ξ_0, fraction F of the 1D Brillouin zone affected by the fluctuations, Cross and Fisher reduced spin-phonon interaction, λ_{CF}, and spin-phonon coupling $|\alpha|$, for $CuGeO_3$, $MEM(TCNQ)_2$, $(TMTTF)_2PF_6$ and $(BCPTTF)_2PF_6$. This table gives also the analog quantities T_P, T_F, Δ, Δ^{MF} (using the expression (6)), Ω_0, Fermi energy E_F, ξ_0 and F for the Peierls transition of TTF-TCNQ and $K_{0.3}MoO_3$. (a), (b) and (c) are respectively the "$2k_F$" frequency of the longitudinal (LA) and transverse (TA) acoustic modes of $MEM(TCNQ)_2$ [74], $TEA(TCNQ)_2$ [86,87] and TTF-TCNQ [69,78].

	T_{SP}(K)	Δ_σ/k_B(K)	T_F(K)	Δ_σ^{MF}/k_B(K)	$\hbar\Omega_0/k_B$(K)	J_{nm}/k_B(K)	ξ_0(Å)	F	λ_{CF}	$\lvert\alpha\rvert/k_B$(K)
$CuGeO_3$	14.3	23–66	60	90	310 (150)	160	4	0.25	0.47	190
$MEM(TCNQ)_2$	18	30	40*	60	100[a]–85[b](LA) ∼ 50[b](TA)	106	Pre-existing Soft mode		0.47	60–90
$(TMTTF)_2PF_6$	19	32	∼80	∼125	80[c](LA) 60[c](TA)	420	14(2)	0.15–0.25	0.24	90–110
$(BCPTTF)_2PF_6$	36	44	100	150	50[c](TA)	330	10(2)	0.25–0.3	0.38	100–125
	T_P(K)	Δ/k_B(K)	T_F(K)	Δ^{MF}/k_B(K)	$\hbar\Omega_0/k_B$(K)	E_F/k_B(K)	ξ_0(Å)	F		
TTF-TCNQ	53	230	150	260	60	910[3]	8(1)	0.4–0.3		
$K_{0.3}MoO_3$	183	870	∼500**	∼880	80	610[3]–10[4]	18(1)	0.1		

∗ In $MEM(TCNQ)_2$, T_F is the temperature at which the critical fluctuations start [18].
∗∗ In $K_{0.3}MoO_3$, T_F is the temperature at which there is a deviation from the linear rate of decrease of the spin susceptibility upon cooling [71].

the charge and spin degrees of freedom and E_F, given by photoemission measurements, plays the role of J_{nn}. Δ^{MF} is deduced from T_F by the BCS relationship [36]:

$$2\Delta^{MF} = 3.52 k_B T_F. \quad (6)$$

In the Peierls systems quoted in Table 1 the lattice and electronic degrees of freedom are well decoupled: $E_F \gg \Delta > \Omega_0$. In addition one has $\Delta \approx \Delta^{MF}$, which shows that these compounds are in the classical limit where there is no important renormalisation of the Peierls gap due to quantum fluctuations. Also a well defined $2k_F$ phonon mode softens. The phonon softening is nearly complete at T_P in $K_{0.3}MoO_3$ [69], where $T_F \gg \Omega_0$. The phonon softening is however incomplete in TTF-TCNQ and the critical growth of a central peak was detected few degrees above T_P [70], recalling the dynamics of the SP chain in the vicinity of the critical ratio R_c. Nevertheless these compounds still belong to the adiabatic limit where the dynamics of the $2k_F$ structural fluctuations are slow enough, with respect to the inverse coherence time of the electronic CDW, to induce a pseudo-gap in the (charge) density of states. The growth of a pseudo-gap has been observed below T_F both in $K_{0.3}MoO_3$ [71] and in TTF-TCNQ.

One has the reverse situation between the lattice and electronic (*i.e.* magnetic) degrees of freedom in $CuGeO_3$. The inequalities $\Omega_0 > J_{nn} > \Delta_\sigma^{MF} > \Delta_\sigma$ place $CuGeO_3$ in the non-adiabatic limit, consistently with the analysis of the lattice dynamics, performed in Section 4, and in agreement with the literature [45,54]. For $CuGeO_3$ we shall consider below Ω_0 only for the $(T_2^+)_1$ mode which has a stronger spin-phonon coupling than the $(T_2^+)_2$ mode, which phonon frequency is indicated in parentheses in Table 1. When the phonon subsystem is faster than the spin subsystem ($\Omega_0 > J_{nn}$) the (temperature dependent) non-adiabatic corrections lead to a renormalisation of the nearest neighbour exchange integral J_{nn} and introduce a next nearest neighbour AF exchange coupling constant J_{nnn} [53]. In this case the spin subsystem can be described by a frustrated Heisenberg AF Hamiltonian which fits nicely the thermal dependence of the spin susceptibility of $CuGeO_3$ [49]. In the non-adiabatic limit the pretransitional fluctuations are too fast to lead to the formation of a pseudo gap in the spin density of states. Indeed in the SP phase of $CuGeO_3$ the gap drops abruptly on heating above 11 K, loosing a factor 2 at T_{SP} [42]. However overdamped gapped excitations can still be guessed slightly above T_{SP} in the 3D critical regime. The unusual thermal behaviour of the gap of $CuGeO_3$ has been explained by invoking either the vicinity of a tricritical point [72,32] or Kosterlitz-Thouless like fluctuations [56].

In $(BCPTTF)_2PF_6$ one has the inequalities: $J_{nn} > \Delta_\sigma^{MF} > \Omega_0 \approx \Delta_\sigma$ which places the compound in the adiabatic limit. Only the first neighbour exchange J_{nn} is required to account for the temperature dependence of the spin susceptibility. According to Figure 4 one expects, with $T_F/\Omega_0 \sim 2 - 1.25$, a soft mode behaviour whose slow fluctuations lead to the development of a pseudo-gap in the (spin) density of states and a drop of the spin

susceptibility below T_F [26]. However the too small crystal size prevents a neutron scattering investigation of the phonon spectrum. In $(BCPTTF)_2PF_6$ the localized limit remains a good approximation because $\Delta_\rho \sim$1000 K is substantially larger than Δ_σ^{MF}. In $(TMTTF)_2PF_6$, with $J_{nn} \gg \Delta_\sigma^{MF} > \Omega_0 > \Delta_\sigma$, there is a better decoupling between the lattice and magnetic degrees of freedom than in $(BCPTTF)_2PF_6$. With $T_F/\Omega_0 \sim 1.6$–1 one still expects, as for $(BCPTTF)_2PF_6$, a soft mode behaviour, and consequently the presence of a pseudo gap. Indeed magnetic measurements reveal its development below 60 K ($\sim T_F$) [16,17]. The decoupling between the charge and spin degrees of freedom is however smaller than in $(BCPTTF)_2PF_6$ because Δ_ρ, of about 300 K according to the recent data of reference [73], is not much larger than Δ_σ^{MF}. As the electrons are only weakly localized, the theory of the SP transition of $(TMTTF)_2PF_6$ should be modified in order to include the itineracy of the charge degrees of freedom (*i.e.* the transfer integral t). This has been performed in reference [7] in the adiabatic limit. However it has been pointed out [4] that near the metal-insulator boundary the successive corrections in t/U can also lead to an effective frustrated Heisenberg coupling between the spin degrees of freedom.

$MEM(TCNQ)_2$, with $J_{nn} > \Delta_\sigma^{MF} \approx \Omega_0 > \Delta_\sigma$, presents a situation intermediate between those of $(BCPTTF)_2PF_6$ and of $CuGeO_3$. $MEM(TCNQ)_2$ is probably just at the boundary between the adiabatic and the non-adiabatic limits. In this respect, the thermal dependence of the spin susceptibility, which is nicely fitted on all the temperature range by the Bonner and Fischer plot [14], indicates neither the formation of a pseudo-gap nor the presence of a sizeable J_{nnn}. The only electronic quantity which shows an anomaly is the thermal dependence of the EPR linewidth which rate of decrease diminishes below T_F [18].The X-ray diffuse scattering investigation [74,18] reveals the existence of a preexisting 3D lattice instability. This instability is already well developped at room temperature. On cooling the associated X- ray diffuse scattering intensity slightly increases, then saturates below 80 K until $T_F \sim 40$ K, temperature below which it diverges [75]. However with a small ratio $T_F/\Omega_0 \sim 1-0.4$ the magnetic chains are probably not able to trig any phonon softening in the acoustic modes of deformation (of bare frequency Ω_0 given Tab. 1); the SP distortion of $MEM(TCNQ)_2$ being acoustic like [76]. This picture is consistent with the non observation of a pseudo-gap. Finally let us recall that, as far as the lattice degrees of freedom are concerned, the SP instability of $MEM(TCNQ)_2$, as well as that of TTF-CuBDT [75], differ from that observed in the others systems where there is a sizeable regime of 1D structural fluctuations which induces a local dimerization coupling progressively first neighbouring spins into a $S = 0$ non-magnetic state. In $MEM(TCNQ)_2$ the SP critical fluctuations grow from a preexiting 2D or 3D lattice instability. It is only at T_F, below T_σ, when the AF correlation length becomes comparable to the structural correlation length of the preexisting soft lattice mode, $\xi_c \sim 17$ Å (*i.e.* $\sim 2c$), that the critical SP regime starts. In $MEM(TCNQ)_2$ ξ_{AF} amounts to about $2c$ at $T_\sigma/2 \sim 35$ K, a temperature close to T_F. At lower temperature the further growth of the magnetic correlations probably drives the divergence of the correlation length of the structural dimerization.

5.2 Spin-phonon coupling

Table 1 gives also the SP coherence length ξ_0 deduced from the experimental data. It is interesting to remark that in $(BCPTTF)_2PF_6$ (10(2) Å/12 Å) and in $(TMTTF)_2PF_6$ (14(2) Å/12 Å) the experimental ξ_0 (left side of the parentheses) agrees within experimental errors with $\xi_0 = \xi_{AF}(T_{SP}^{MF})$ calculated from the expression (1) (right side of the parentheses). In $MEM(TCNQ)_2$, ξ_0 calculated with T_F is two times smaller than ξ_c measured at T_F, which again points out for the existence of a different mechanism for the SP transition.

With these ξ_0 values it is possible to define the fraction, F, of the 1D Brillouin zone, associated to the chain repeat unit, which is affected by the fluctuations and thus to determine which (weak or strong?) spin-phonon coupling limit is the most appropriate to describe the SP transition. This fraction is simply given, Table 1, by the quantity $F = 2(\xi_0 G_\parallel)^{-1}$, where ξ_0 is the above quoted coherence length, when the critical wave vector, q_c, is at the Brillouin zone boundary ($q_c = G_\parallel/2$ for a SP instability). In a comparison purpose Table 1 gives also F for the two Peierls systems previously considered. However in that case F is two time larger because $q_c = 2k_F$ being inside the Brillouin zone both the $+2k_F$ and $-2k_F$ critical wave vectors of the fluctuations have to be counted. In the case of a $2k_F$ phonon softening this fraction, F, can be alternatively given by the ratio $4\Delta_q/G_\parallel$, where Δq is the full width at half maximum of the Kohn anomaly. If $F \ll 1$, few phonon modes are involved in the SP or Peierls instability. The phonon entropy can be neglected, and thus the transition is described by the BCS weak coupling mean-field scenario, if one neglects the 1D lattice fluctuations. In this scenario the SP or Peierls gap and the critical temperature are related respectively by the relationships (2) or (6). This scenario holds for the blue bronze $K_{0.3}MoO_3$, where $F \sim 0.1$. In the opposite limit where $F \sim 1$, the instability nucleates from a local distortion, whose size is given ξ_0, and there are thus so much phonon modes involved that one cannot neglect the lattice entropy. This implies a strong coupling scenario between the electronic and lattice degrees of freedom. TTF-TCNQ, with $F \sim 0.4-0.3$, is not too far from this limit. Similar values of F are found in the transition metal dichalcogenides, such as 2H-$TaSe_2$ and 2H-$NbSe_2$, for which a strong coupling theory of the Peierls transition has been performed [77]. This strong coupling theory gives an enhancement of the Peierls gap and thus the BCS relationship (6) no longer hold: the Δ^{MF}/T_P^{MF} ratio is enhanced with respect to the BCS ratio. Table 1 shows that, with $F \sim 0.25$, $CuGeO_3$ is in the intermediate coupling regime. This seems also to be the case for $(BCPTTF)_2PF_6$ and $(TMTTF)_2PF_6$.

Alternatively, the spin-phonon coupling can be obtained under a reduced form, $\lambda_{\rm CF}$, from the mean-field expression of Cross and Fischer [59]:

$$k_{\rm B}T_{\rm SP}^{\rm MF} = 0.8J_{nn}\lambda_{\rm CF}. \quad (7)$$

$\lambda_{\rm CF}$ is given in Table 1 for the different SP systems. It shows that $CuGeO_3$ is in the intermediate coupling regime, as $MEM(TCNQ)_2$. The coupling appears to be smaller in $(BCPTTF)_2$ PF_6 and in $(TMTTF)_2$ PF_6. From the relationship:

$$\lambda_{\rm CF} = 2\alpha^2/(\pi J_{nn}\Omega_0) \quad (8)$$

one can deduces (Table 1) the absolute value of the spin-phonon coupling $|\alpha|$. In $CuGeO_3$ $|\alpha|$ is comparable to J_{nn}, and about two times larger than the mean field gap $\Delta_\sigma^{\rm MF}$. Our determination gives a $|\alpha|$ value two times larger that the one deduced from the mean-field analysis of reference [31] where the lower bound of Δ_σ was used instead of $\Delta_\sigma^{\rm MF} \approx 0.8\alpha^2/\Omega_0$ [43]. In $(BCPTTF)_2$ PF_6 and $(TMTTF)_2$ PF_6 $|\alpha|$ amounts to about $J_{nn}/3$ and $J_{nn}/4$ respectively, and is comparable to $\Delta_\sigma^{\rm MF}$.

5.3 Spin-Peierls ground state

In the localized limit, the $T = 0$ K SP phase diagram depends upon the reduced variables α/J_{nn} and Ω_0/J_{nn}. The boundary between the classical and quantum gapped phases, as well as the gapped-ungapped quantum critical boundary, have been determined for the XY-SP chain coupled with "site phonons" [8] but only the latter critical boundary is available for the Heisenberg-SP chain coupled with "site phonons" [10] or "bond phonons" [67]. According to Figure 2 in reference [8], the data of Table 1 indicate that:

- $CuGeO_3$, as well as $MEM(TCNQ)_2$, are inside the quantum gapped state, with $CuGeO_3$ closer to the quantum gapless boundary than $MEM(TCNQ)_2$,
- $(BCPTTF)_2PF_6$ and $(TMTTF)_2PF_6$ are on the classical-quantum boundary in the gapped state.

With the spin-phonon Hamiltonian considered in reference [10] $CuGeO_3$ is inside the quantum gapped state, while for that of reference [67] $CuGeO_3$ is at the quantum gapless boundary [88].

Our analysis places $CuGeO_3$ both in the intermediate coupling regime and in the non-adiabatic limit, as previously reported in the literature [45]. However while a strengthening of the coupling enhances the SP gap, the non-adiabatic corrections tends to depress it. The location of $CuGeO_3$ in the quantum region very near the critical boundary to the gapless quantum region, corresponding to the critical spin-phonon coupling $\alpha_{\rm c}$, means that the non-adiabatic corrections are the strongest. In presence of quantum fluctuations the 1D-SP gap should vary exponentially with $|\alpha - \alpha_{\rm c}|$ [8,10]. In this respect it is interesting to remark that with the microscopic constants of Table 1 one finds, from the calculation of reference [10] performed with $\Omega_0 = J_{nn}$, that the spin Peierls gap of $CuGeO_3$, Δ_σ, amounts at about half its mean field value, $\Delta_\sigma^{\rm MF}$. This is in agreement with the ratio of the gaps quoted Table 1.

Using the calculations of reference [46], performed with $\Omega_0 = 0.3J_{nn}$, and the microscopic constants of Table 1 one obtains a singlet-triplet gap of $\Delta_\sigma \approx 35$ K for $(TMTTF)_2PF_6$ and of $\Delta_\sigma \approx 55$ K for $(BCPTTF)_2PF_6$. These calculated values are in quite good agreement with the experimental ones deduced from the thermal dependence of the spin susceptibility below $T_{\rm SP}$ (32 K [17] and 44 K [89] respectively – see Table I).

5.4 Pressure dependence

It is interesting to remark that the SP critical temperature varies strongly under pressure. $T_{\rm SP}$ increases sizeably in $CuGeO_3$ (dLog $T_{\rm SP}/{\rm d}p$ amounts to +25%/GPa [79,80,51]) and in $MEM(TCNQ)_2$ (+100%/GPa [81]). Contrarily, $T_{\rm SP}$ of $(TMTTF)_2PF_6$ decreases strongly under pressure (−30%/GPa). However the phase diagram of this latter compound is quite complex with the presence of several ordered states competing with the SP phase [82]. In these SP compounds the rate of variation of $T_{\rm SP}$ is much stronger than the one observed in the Peierls systems (+9%/GPa in TTF-TCNQ, −8%/GPa in $K_{0.3}MoO_3$).

As in any 1D system, the $T_{\rm SP}$ variation is due to the combined effect of the variations of the interchain coupling and of the intrachain interactions. Basically one has [36]:

$$k_{\rm B}T_{\rm SP} \approx zC_\perp\xi_c(T_{\rm SP})/c, \quad (9)$$

where $C_\perp$ is the interchain coupling energy, z is the number of neighbouring chains and $\xi_c(T)$ is the intrachain correlation length (shown Fig. 3 in function of $T_{\rm SP}^{\rm MF} = 0.57\alpha^2/\Omega_0$ and of $\xi_0 = cJ_{nn}/2k_{\rm B}T_{\rm SP}^{\rm MF}$). All these quantities can vary under pressure. Thus one has to consider, in addition to the probable increase of $C_\perp$ under pressure, the pressure dependence of the intrachain interactions. Generally Ω_0 increases under pressure (${\rm dLog}\Omega_0/{\rm d}p > 0$) [51]. In $CuGeO_3$ the pressure dependence of the first neighbour exchange integral is negative, ${\rm dLog}J_{nn}/{\rm d}p = -7\%$/GPa, while that of J_{nnn} can be neglected [49]. The pressure dependence of α is more difficult to evaluate. With $\alpha \propto \nabla J/\sqrt{\Omega_0}$, one obtains:

$${\rm dLog}|\alpha|/{\rm d}p = {\rm dLog}J/{\rm d}p - 0.5{\rm dLog}\Omega_0/{\rm d}p, \quad (10)$$

if one assumes that J decreases exponentially with the distance ($\nabla J \propto -J$). With (10) one gets:

$${\rm dLog}T_{\rm SP}^{\rm MF}/{\rm d}p = 2({\rm dLog}J/{\rm d}p - {\rm dLog}\Omega_0/{\rm d}p), \quad (11)$$

and:

$${\rm dLog}\xi_0/{\rm d}p = -{\rm dLog}J/{\rm d}p + 2{\rm dLog}\Omega_0/{\rm d}p. \quad (12)$$

The rate of variation of these quantities is determined by differences between dLogJ/dp and ${\rm dLog}\Omega_0/{\rm d}p$. If one assumes that the hydrostatic pressure dependence of $|\alpha|$ in $CuGeO_3$ is simply given by the expression (10), the negative pressure dependence of J_{nn} leads to a decrease of $|\alpha|$.

Then expressions (11) and (12) show that T_{SP}^{MF} decreases and ξ_0 increases under pressure. As T_{SP} occurs in the solitonic regime of $\xi_c(T)$, one gets from the expression (4):

$$\mathrm{dLog}\xi_c(T)/\mathrm{d}p = \mathrm{dLog}\xi_0/\mathrm{d}p + [a(T_{SP}^{MF}/T) - 1]\mathrm{dLog}T_{SP}^{MF}/\mathrm{d}p, \quad (13)$$

which gives for $T_{SP} \approx T_{SP}^{MF}/4$:

$$\mathrm{dLog}\xi_c(T_{SP})/\mathrm{d}p \approx 5\mathrm{dLog}J/\mathrm{d}p - 4\mathrm{dLog}\Omega_0/\mathrm{d}p. \quad (14)$$

This expression shows that $\xi_c(T_{SP})$ decreases under pressure. Thus the pressure increase of T_{SP}, given by the expression (9), can be attributed to the increase of $C_\perp$.

However since J_{nn}/Ω_0 decreases under pressure, α_c/Ω_0 must decrease too [10]. As $|\alpha|/\Omega_0$ behaves similarly, it is important to determine how the difference $|\alpha-\alpha_c|/\Omega_0$ varies under pressure because the increase (decrease) of $|\alpha-\alpha_c|$ leads to an increase (decrease) of the 1D-SP gap. A possible answer can be brought by the pressure dependence of the singlet-triplet dispersion curve. The measurements of reference [44] show that the lowest value of the singlet-triplet excitation energy of $CuGeO_3$ exhibits a rate of increase of +65%/GPa, more than two times stronger than T_{SP}! This means either (i) that the dispersion along b^* of the singlet-triplet excitation band (which spreads on 43 K at ambient pressure) decreases under pressure or/and (ii) that its mid-band value, which has been identified at Δ_σ in this paper, increases under pressure. Let us first examine the first scenario (i). Usually one expects, with the increase of the interchain coupling, an increase of the dispersion under pressure. The opposite behavior should indicate that the b^* dispersion is not due to a simple interchain exchange coupling but more likely that the anomalous pressure dependence of the singlet-triplet excitation energy, at the AF critical wave vector, could reflect a frequency softening related to an incipient AF instability. In this scenario, by extrapolating the pressure variation of its energy, one expects the vanishing of the AF gap under a negative pressure of −1.5 GPa. At this pressure, the AF ground state should be stabilized and one should have $\alpha = \alpha_c$. This scenario is consistent with the conclusions of the previous section placing $CuGeO_3$ very close to the quantum gapless boundary. The pressure thus would control the AF-SP phase diagram through the variation of $|\alpha-\alpha_c|$. In the second scenario (ii), which is not incompatible with the first one, the increase of the mid-band energy under pressure means an increase of the 3D-SP gap. The increase of the 3D-SP gap under pressure is consistent with the increase of T_{sp}. The increase of the 3D-SP gap can be both attributed to the increase of $|\alpha - \alpha_c|$, which leads to an increase of the 1D-SP gap, and to the increase of the interchain coupling $C_\perp$. The enhancement of the 1D-SP gap could be due to the reduction of the quantum fluctuations present in the vicinity of the quantum critical point, α_c, of the SP chain (for a general review on the quantum criticality see Ref. [83]).

6 Conclusion

From the study of the pretransitional lattice fluctuations we have been able to determine a set of microscopic parameters which describe consistently the mechanism of the SP transition of $CuGeO_3$. We have also compared these parameters with those of the others organic SP systems. We found that $(BCPTTF)_2PF_6$ and $(TMTTF)_2PF_6$ are located in the adiabatic limit, that $CuGeO_3$ is in the non-adiabatic limit and that $MEM(TCNQ)_2$ is at the boundary between these two limits. $(BCPTTF)_2PF_6$ and $(TMTTF)_2PF_6$ are situated on the SP gapped classical-quantum boundary, $MEM(TCNQ)_2$ is in the quantum SP gapped phase, while $CuGeO_3$ is also in this latter phase but closer to the quantum gapless boundary.

The location of $CuGeO_3$ near a quantum critical point, α_c, could facilitate the switch between the gapped SP state and the gapless AF state. As α decreases and crosses the critical quantum point α_c there is a drop of order parameter indicating the closing of the spin gap. When the low energy excitations are described by the sine-Gordon model [84], which is the case for the generation of solitons in the SP chain, a Kosterlitz-Thouless (KT) type transition occurs at α_c. This KT transition has a hidden SU(2) symmetry: at the transition the correlation length is very singular (exponential dependence with a power of $|\alpha-\alpha_c|$), and for α slightly larger than α_c, the 1D SP gap is an exponentially small quantity of $|\alpha - \alpha_c|$.

In the vicinity of α_c the stabilization of the SP state should depend strongly upon the interchain coupling and upon the perturbations induced by the atomic substituents. This is probably a key feature for the interpretation of the phase diagram of $CuGeO_3$ which is governed by the competition between the gapped SP state and the gapless AF state. In this respect it is now established that an extremely small amount of substituent gives rise to the coexistence between 3D SP and AF orders [85]. We shall discuss the effect of substituents on the SP transition of $CuGeO_3$ in a companion paper [63].

At finite temperature in the quantum region near α_c one should also expect anomalous variations of the order parameter reflecting the presence of KT type fluctuations. This could provide an alternative explanation at the unusual thermal temperature dependence of the SP order parameter in $CuGeO_3$ [56]. The physical quantities measured in the vicinity of a critical quantum point, which depend upon the microscopic parameters through the difference $|\alpha - \alpha_c|$, are not universal. This statement could thus appear to be in contradiction with the use of a "universal" behaviour to interpret the thermal dependence of the intrachain correlation length (Fig. 3). However a 1D quantum-classical crossover is expected when the temperature exceeds $k_B T_{QC} \approx \Delta_\sigma/\pi$ (*i.e.* when the thermal coherence length is smaller than the quantum coherence length associated to the critical point). By taking $\Delta_\sigma \approx 45$ K, the crossover temperature is estimated at $T_{QC} \sim 14\,\mathrm{K} \approx T_{SP}$. In this picture the pretransitional fluctuations will be in the classical "universal" regime while the SP ground state will be in the quantum regime.

This paper is written in memory of Heinz Schulz. It was always a pleasure and a great mutual benefit to discuss physics with Heinz. Figure 4 was issued from an unpublished calculation of Heinz. I thank also Professor J. Friedel for comments on the manuscipt and S. Ravy for usefull discussions.

Note added in proof

After acceptation of the paper, Nishi *et al.* reported [abstract L31-5, Bull. Am. Phys. Soc. **46**, 524 (2001)] that the zone center b*-longitudinal optical phonon mode of energy of 0.9 meV, which involves the tilt of the O(2)-O(2) squares [see Nishi *et al.* J. Phys. Chem. Solids **60**, 1109 (1999)], exhibits below 60 K an anomalous decrease of intensity. Such a decrease could correspond to a huge enhancement of the Debye Waller factor of its inelastic structure factor. This enhancement itself could be provoked by a large increase of the mean square O(2) displacement due to the development below $T_{\rm SP}^{\rm MF}$ of the critical fluctuations of the $(\mathrm{T}_2^+)_2$ SP order parameter.

References

1. J. Voit, Rep. Prog. Phys. **58**, 977 (1995).
2. H.J. Schulz, G. Cuniberti, P. Pieri, in *Field Theories for Low-Dimensional Condensed Matter Systems*, edited by G. Morandi *et al.* (Springer, 2000), `cond-mat/9807366`.
3. P.W. Anderson, Mater. Res. Bull. **8**, 153 (1973).
4. See, for example, H. Fukuyama, Synth. Met **19**, 63 (1987).
5. G.S. Uhrig, H.J. Schulz, Phys. Rev. B **54**, R9624 (1996).
6. E. Pytte, Phys. Rev. B **10**, 4637 (1974).
7. C. Bourbonnais, B. Dumoulin, J. Phys. I France **6**, 1727 (1996).
8. L.G. Caron, S. Moukouri, Phys. Rev. Lett. **76**, 4050 (1996).
9. A.W. Sandvik, D.K. Campbell, Phys. Rev. Lett. **83**, 195 (1999).
10. R.J. Bursill, R.H. McKenzie, C.J. Hamer, Phys. Rev. Lett. **83**, 408 (1999).
11. J.P. Pouget, H. Launois, T.M. Rice, P. Dernier, A. Gossard, G. Villeneuve, P. Hagenmuller, Phys. Rev. B **10**, 1801 (1974).
12. J.W. Bray, H.R. Hart, L.V. Interrante, I.S. Jacobs, J.S. Kasper, G.D. Watkins, S.H. Wee, J.C. Bonner, Phys. Rev. Lett. **35**, 744 (1975).
13. M. Hase, I. Terasaki, K. Uchinokura, Phys. Rev. Lett. 70, 3651 (1993); M. Hase, I. Terasaki, K. Uchinokura, Phys. Rev. Lett. **70**, 3651 (1993).
14. S. Huzinga, J. Kommandeur, G.A. Sawatzky, B.T. Thole, K. Kopinga, W.J.M. De Jonge, J. Roos, Phys. Rev. B **19**, 4723 (1979).
15. J.P. Pouget, R. Moret, R. Comes, K. Bechgaard, J.M. Fabre, L. Giral, Mol. Cryst. Liq. Cryst. **79**, 129 (1982).
16. F. Creuzet, C. Bourbonnais, L.G. Caron, D. Jérome, K. Bechgaard, Synth. Met. **19**, 299 (1987).
17. M. Dumm, A. Loidl, B.W. Fravel, K.P. Starkey, L.K. Montgomery, M. Dressel, Phys. Rev. B **61**, 511 (2000).
18. Q. Liu, S. Ravy, J.P. Pouget, C. Coulon, C. Bourbonnais, Synth. Met. **55–57**, 1840 (1993).
19. Y. Ueda, Chem. Mater. **10**, 2653 (1998).
20. J. Riera, D. Poilblanc, Phys. Rev. B **59**, 2667 (1999).
21. K.C. Ung, S. Mazumdar, D. Toussaint, Phys. Rev. Lett. **73**, 2603 (1994).
22. S. Mazumdar, R.T. Clay, D.K. Campbell, Phys. Rev. B **62**, 13400 (2000).
23. J. Riera, D. Poilblanc, Phys. Rev. B **62**, R16243 (2000).
24. A.J. Heeger, S. Kivelson, J.R. Schrieffer, W.-P. Su, Rev. Mod. Phys. **60**, 781 (1988).
25. B. Dumoulin, thesis (University of Sherbrooke, Canada, 1997). The expression (3) is obtained from an empirical fit of the numerical calculation with a mean field like square root thermal dependence. The expression (4) is obtained by the conventional WKB method (see J.A. Krumhansl, J.R. Schrieffer, Phys. Rev. B **11**, 3535 (1975) and J.F. Curie *et al.*, Phys. Rev. B **22**, 477 (1980)).
26. B. Dumoulin, C. Bourbonnais, S. Ravy, J.P. Pouget, C. Coulon, Phys. Rev. Lett. **76**, 1360 (1996).
27. J.W. Bray, Solid State Commun. **26**, 771 (1978).
28. L.N. Bulaevskii, A.I. Buzdin, D.I. Khomskii, Solid State Commun. **27**, 5 (1978).
29. A. Buzdin, M.L. Kulic, V.V. Tugushev, Solid State Commun. **48**, 483 (1983).
30. M. Mostovoy, D. Khomskii, Z. Phys. B **103**, 209 (1997).
31. R. Werner, C. Gros, M. Braden, Phys. Rev. B **59**, 14356 (1999).
32. R. Werner, C. Gros, Phys. Rev. B **57**, 2897 (1998).
33. C. Gros, R. Werner, Phys. Rev. B **58**, R14677 (1998).
34. A. Klümper, R. Raupach, F. Schönfeld, Phys. Rev. B **59**, 3612 (1999).
35. (a) M. Holicki, H. Fehske, R. Werner, `cond-mat/0006169`; (b) R. Werner, `cond-mat/0006168`.
36. See for example D. Jérome, H.J. Schulz, Adv. Phys. **31**, 299 (1982).
37. J.P. Pouget, L.P. Regnault, M. Ain, B. Hennion, J.P. Renard, P. Veillet, G. Dhalenne, A. Revcolevscki, Phys. Rev. Lett. **72**, 4037 (1994).
38. J.P. Schoeffel, J.P. Pouget, G. Dhalenne, A. Revcolevschi, Phys. Rev. B **53**, 14971 (1996). In Figure 5 of this paper ξ_b^{-1} was incorrectly reported at 19.5 K with a value two times smaller than experimentally measured. This error is corrected in Figure 2 of the present paper.
39. O. Kamimura, M. Terauchi, M. Tanaka, O. Fujita, J. Akimitsu, J. Phys. Soc. Jpn **63**, 2467 (1994).
40. K. Hirota, D.E. Cox, J.E. Lorenzo, G. Shirane, J.M. Tranquada, M. Hase, K. Uchinokura, H. Kojima, Y. Shibuya, I. Tanaka, Phys. Rev. Lett. **73**, 736 (1994).
41. M. Braden, G. Wilkendorf, J. Lorenzana, M. Ain, G. J. McIntyre, M. Behruzi, G. Heger, G. Dhalenne, A. Revcolevschi, Phys. Rev. B **54**, 1105 (1996).
42. J.P. Boucher, L.P. Regnault, J. Phys. I France **6**, 1939 (1996).
43. H.J. Schulz, in *Low-Dimensional Conductors and Superconductors*, edited by D. Jérome, L.G. Caron, NATO ASI B **155** (Plenum Press, New-York, 1987), p. 95.
44. M. Nishi, O. Fujita, J. Akimitsu, K. Kakurai, Y. Fujii, Phys. Rev. B **52**, R6959 (1995).
45. G. Wellein, H. Fehske, A.P. Kampf, Phys. Rev. Lett. **81**, 3956 (1998).
46. D. Augier, D. Poilblanc, E. Sørensen, I. Affleck, Phys. Rev. B **58**, 9110 (1998); D. Augier, D. Poilblanc Eur. Phys. J. B **1**, 19 (1998).

47. J. Riera, A. Dobry, Phys. Rev. B **51**, 16098 (1995).
48. G. Castilla, S. Chakravarty, V.J. Emery, Phys. Rev. Lett. **75**, 1823 (1995).
49. K. Fabricius, A. Klümper, U. Löw, B. Büchner, T. Lorenz, G. Dhalenne, A. Revcolevschi, Phys. Rev. B **57**, 1102 (1998).
50. B. Büchner, U. Ammerahl, T. Lorenz, W. Brenig, G. Dhalenne, A. Revcolevschi, Phys. Rev. Lett. **77**, 1624 (1996).
51. P.H.M. van Loosdrecht, J. Zeman, G. Martinez, G. Dhalenne, A. Revcolevschi, Phys. Rev. Lett. **78**, 487 (1997).
52. H. Yokoyama, Y. Saiga, J. Phys. Soc. Jpn **66**, 3617 (1997).
53. K. Kukobi, H. Fukuyama, J. Phys. Soc. Jpn **56**, 3126 (1987); G.S. Uhrig, Phys. Rev. B **57**, R14004 (1998). See also A. Weisse, G. Wellein, H. Fehske, `cond-mat/9901262` for a corrected version.
54. R.W. Kühne, U. Löw, `cond-mat/9905337`.
55. K. Hirota, G. Shirane, Q. J. Harris, Q. Feng, R.J. Birgeneau, M. Hase, K. Uchinokura, Phys. Rev. B **52**, 15412 (1995).
56. J.E. Lorenzo, L.P. Regnault, S. Langridge, C. Vettier, C. Sutter, G. Grübel, J. Souletie, J.G. Lussier, J.P. Schoeffel, J.P. Pouget, A. Stunault, D. Wremeille, G. Dhalenne, A. Revcolevschi, Europhys. Lett. **45**, 45 (1999).
57. Y.J. Wang, Y.-J. Kim, R.J. Christianson, S.C. LaMarra, F.C. Chou, R.J. Birgeneau, Phys. Rev. B **63**, 052502 (2001).
58. S. Ravy, J. Jegoudez, A. Revcolevschi, Phys. Rev. B **59**, R681 (1999).
59. M.C. Cross, D.S. Fisher, Phys. Rev. B **19**, 402 (1979).
60. H. Winkelmann, E. Gamper, B. Büchner, M. Braden, A. Revcolevschi, G. Dhalenne, Phys. Rev. B **51**, 12884 (1995).
61. M. Poirier, R. Beaudry, M . Castonguay, M.L. Plumer, G. Quirion, F.S. Razavi, A. Revcolevschi, G. Dhalenne, Phys. Rev. B **52**, R6971 (1995).
62. M. Horvatic, Y. Fagot-Revurat, C. Berthier, G. Dhalenne, A. Revcolevschi, Phys. Rev. Lett. **83**, 420 (1999).
63. J.P. Pouget, J.P. Schoeffel, G. Dhalenne, A. Revcolevschi (in preparation).
64. M. Braden, B. Hennion, W. Reichardt, G. Dhalenne, A. Revcolevschi, Phys. Rev. Lett. **80**, 3634 (1998).
65. L.P. Regnault, F. Tasset, J.E. Lorenzo, T. Roberts, G. Dhalenne, A. Revcolevschi (to be published).
66. H.J. Schulz (unpublished, 1997). The calculation is performed for a spinless Luttinger liquid coupled to a 3D phonon field with a (steep) transverse dispersion. The correlation functions of the Heisenberg model corresponds to those of this Luttinger liquid with the exponent $K = 1/2$ (see [2] for example).
67. D. Augier, thesis (University of Toulouse, France, 1999). See Figure II.24 in particular.
68. E. Tutis, S. Barisic, Phys. Rev. B **43**, 8431 (1991).
69. J.P. Pouget, B. Hennion, C. Escribe-Filippini, M. Sato, Phys. Rev. B **43**, 8421 (1991).
70. G. Shirane, S.M. Shapiro, R. Comès, A.F. Garito, A.J. Heeger, Phys. Rev. B **14**, 2325 (1976); R. Comès, G. Shirane, S.M. Shapiro, A.F. Garito, A.J. Heeger, Phys. Rev. B **14**, 2376 (1976).
71. D.C. Johnston, Phys. Rev. Lett. **52**, 2049 (1984).
72. R.J. Birgeneau, V. Kiryukhin, Y.J. Wang, Phys. Rev. B **60**, 14816 (1999).
73. F. Nad, P. Monceau, C. Carcel, J.M. Fabre, Phys. Rev. B **62**, 1753 (2000).
74. B. van Bodegom, B.C. Larson, H.A. Mook, Phys. Rev. B **24**, 1520 (1981).
75. The thermal variation of the X-ray diffuse scattering intensity corrected by the thermal population factor measured in TTF-CuBDT (D.E. Moncton *et al.*, Phys. Rev. Lett. **57**, 507 (1977)) behaves similarly as in $MEN(TCNQ)_2$. It varies weakly upon cooling until about $T_F \sim 40$ K ($< T_\sigma = 50$ K), temperature below which it starts to diverge critically down to $T_{SP} = 11$ K.
76. R.J. Visser, S. Oostra, C. Vettier, J. Voiron, Phys. Rev. B **28**, 2074 (1983).
77. W.L. McMillan, Phys. Rev. B **16**, 643 (1977).
78. J.P. Pouget, S.M. Shapiro, G. Shirane, A.F. Garito, A.J. Heeger, Phys. Rev. B **19**, 1792 (1979).
79. H. Takahashi, N. Môri, O. Fujita, J. Akimitsu, T. Matsumoto, Solid State Commun. **95**, 817 (1995).
80. A.R. Gońi, T. Zhou, U. Schwarz, R.K. Kremer, K. Syassen, Phys. Rev. Lett. **77**, 1079 (1996).
81. D. Bloch, J. Voiron, C. Vettier, J.W. Bray, S. Oostra, J. Phys Colloq. **44**, C3-1317 (1983) and Physica B **119**, 43 (1983).
82. C. Bourbonnais, D. Jérome, in *Advances in Synthetic Metals ; Twenty Years of Progress in Science and Technology*, edited by P. Bernier, E. Lefrant, G. Bidan (Elsevier, 1999), Chap. 3, p. 206.
83. S. Sachdev, Phys. World **12**, 33 (1999); Science **288**, 461 (2000).
84. K. Numora, K. Okamoto, J. Phys. A **27**, 5773 (1994).
85. B. Grenier, J.P. Renard, P. Veillet, C. Paulsen, G. Dhalenne, A. Revcolevschi, Phys. Rev. B **58**, 8202 (1998).
86. K. Carneiro, M. Almeida, L. Alcacer, Solid State Commun. **44**, 959 (1982).
87. J.S. Pedersen, K. Carneiro, M. Almeida, J. Phys. C **20**, 1781 (1987).
88. The spin-phonon Hamiltonians involving the "site phonons" and the "bond phonons" have, for the phonon counterpart, the same expression as the electron-phonon Hamiltonians entering respectively in the SSH and Holstein Hamiltonians of the Peierls transition.
89. C. Coulon (private communication).